

Title: Seismic Performance Assessment of Eurocode 8-Compliant Concentric Braced Frame Buildings Using FEMA P-58

Authors: Giuseppe Marcantonio Del Gobbo^{1†}, Martin S. Williams², Anthony Blakeborough³

¹ Department of Engineering Science, University of Oxford, Parks Road, Oxford, OX1 3PJ
giuseppe.delgobbo@eng.ox.ac.uk

† Corresponding author

² Department of Engineering Science, University of Oxford, Parks Road, Oxford, OX1 3PJ
martin.williams@eng.ox.ac.uk

³ Department of Engineering Science, University of Oxford, Parks Road, Oxford, OX1 3PJ
tony.blakeborough@eng.ox.ac.uk

Title: Seismic Performance Assessment of Eurocode 8-Compliant Concentric Braced Frame Buildings Using FEMA P-58

Abstract: Damage to nonstructural systems during recent earthquakes has resulted in costly repairs and extended building downtime. Achieving a desired seismic performance requires the coordination of structural and nonstructural performance. Eurocode 8 prescribes interstorey drift limits with the aim of controlling nonstructural damage, but a better understanding of the effectiveness of this approach is needed. This study assesses the seismic performance of Eurocode-compliant concentric braced frame buildings designed to meet different drift limits. The FEMA P-58 procedure is used to estimate repair costs. The assessments indicated that many structures designed to modern standards may be demolished following a ULS earthquake due to the high repair costs. Substantial SLS repair costs are also expected. The majority of repair costs can be attributed to nonstructural systems. Storeys satisfying the Eurocode drift limit nevertheless experienced both drift-sensitive and acceleration-sensitive nonstructural damage. Although codes focus on drifts when considering nonstructural response, acceleration-sensitive damage is of comparable or greater consequence than drift-sensitive damage. The repair cost calculations were found to be sensitive to nonstructural quantities and nonstructural elements' seismic design categorization. The results suggest that modern building standards do not reliably deliver earthquake resilience.

Keywords: Eurocode; FEMA P-58; Concentric Braced Frames; Nonstructural Systems; Seismic Performance Assessment

1 Introduction

Nonstructural systems are essential to building operations and comprise the majority of building investment [1]. Damage to nonstructural systems during recent earthquakes has resulted in costly repairs and extended building downtime [2–4]. Achieving a desired seismic performance requires the coordination of structural and nonstructural performance, and an improved understanding of the total-building seismic performance of conventional code-compliant structures is therefore needed.

Most previous research on Eurocode concentric braced frame (CBF) buildings has focused on structural performance. The determination of total-building seismic performance considering nonstructural systems has not been evaluated in detail. In addition, the applicability of the Eurocode 8 drift limits for nonstructural damage remains uncertain.

Previous studies comparing seismic performance consider structural parameters such as interstorey drifts and floor accelerations [5,6]. Complexities arise as these parameters are

often competing objectives. Limitations are introduced when determining appropriate parameter weights to represent performance. Other studies use damage indices that are influenced by several assumptions to represent performance [7,8]. The use of repair costs is a more appropriate measure of total-building seismic performance and avoids these limitations.

This study assesses the seismic performance of Eurocode 8-compliant CBF structures that are representative of buildings constructed in seismic regions. The structures are designed to meet drift performance limits in accordance with Eurocode 8 [9], which prescribes interstorey drift limits to control nonstructural damage. The effectiveness of the Eurocode nonstructural damage methodology is investigated through seismic performance assessments. These performance assessments also provide a benchmark on which to evaluate retrofit alternatives for existing buildings or design options for new structures.

Finite element models are created in OpenSees [10] to determine structural response. The FEMA P-58 procedure [11] is used to translate the structural response parameters to expected repair costs. Sensitivity studies are conducted to characterize the sensitivity of FEMA P-58 repair cost calculations to typical assumptions.

2 Methodology

The study comprises the following steps, described more fully below: selection of desired structural properties, design of a suite of steel CBF buildings using Eurocode 8, nonlinear modelling of the buildings using OpenSees, creation of ground motion suites for time history analysis, and modification and implementation of the FEMA P-58 assessment procedure.

2.1 Description of Study Buildings

The buildings used in this study are representative of structures designed using modern codes for regions with significant seismic hazard. The scope of the investigation is limited to steel CBF office buildings. Braced steel frames are a common design type and can also be used to accommodate dampers [12]. The Eurocode standards [13] were selected for design. 4-storey, 8-storey and 16-storey structures with storey heights of 3.5m were designed.

Eurocode 8 Cl 4.4.3 [9] specifies damage limitation requirements as interstorey drift limits based on the composition of nonstructural systems in the building. The strictest drift limit “for buildings having non-structural elements of brittle materials” is $d_r v \leq 0.005h$, where d_r is the design interstorey drift, h is the storey height and v is a reduction factor (0.5 for Importance Class II) based on the lower return period of the damage limitation earthquake. Serviceability is expected at 0.5% drift according to the Eurocode methodology. One set of buildings was designed to meet the 0.5% drift criterion during the SLS, referred to as 4S, 8S and 16S for the 4-storey, 8-storey, and 16-storey structures respectively. These designs represent the maximum performance of Eurocode-compliant structures.

There is a growing interest in performance-based design and achieving resiliency during structural design. Current code provisions impose stringent drift limits with the objective of reducing damage. A second set of buildings was designed to achieve beyond-code performance, while still applying the Eurocode approach. A 4-storey and an 8-storey structure were designed to meet the Eurocode serviceability 0.5% drift criterion during the ULS, referred to as 4D and 8D respectively. The advanced drift criterion was unable to be met feasibly for the 16-storey building using CBFs; brace sections could not be selected that achieved 0.5% ULS drift and met the Eurocode steel design requirements without an impractical number of braced bays. Elevation views of the structures are shown in Figure 1.

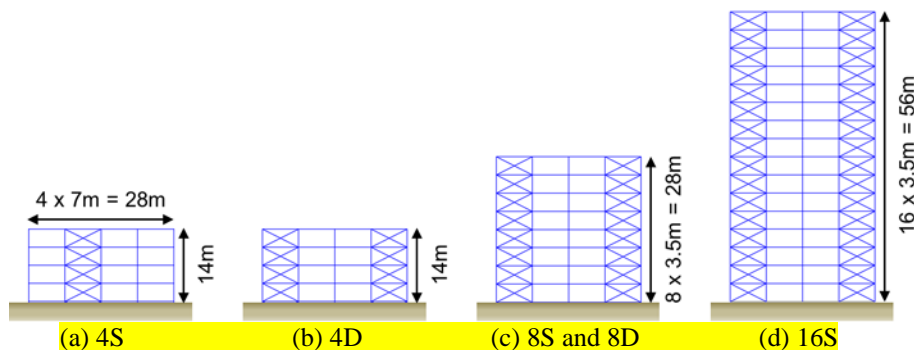


Figure 1: Elevation views of the office buildings

Pinned beam-column and beam-beam connections are used. The columns are continuous over several storeys with rigid splices and are pinned at base level. The brace

members are pinned. Buildings 4D, 8S, 8D and 16S have four braced bays in each direction. Building 4S only required two braced bays in each direction to meet the drift limit. Plan views of the structures are shown in Figure 2.

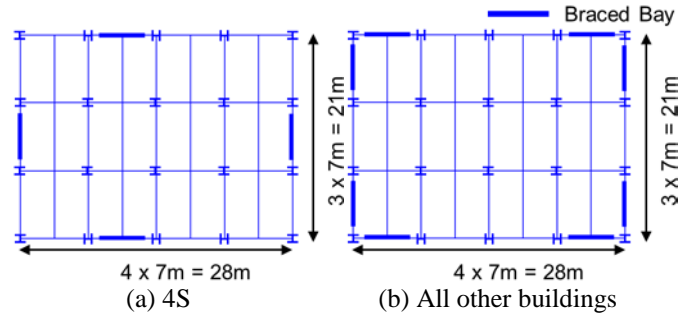


Figure 2: Plan views of the office buildings

2.2 Building Design

The office buildings are designed to resist dead, imposed, snow, wind and seismic loads using the Eurocodes [9,13–15]. Dead loads considered in the design include the self-weight of structural members as well as allowances for nonstructural components such as cladding, suspended ceilings, floor finishes, and mechanical, electrical and plumbing systems ($DL = 4.47\text{kN/m}^2$). The imposed loads correspond to office use (Category B1) while the intermediate partition load value was assumed ($IL = 3.3\text{kN/m}^2$). The Type One horizontal elastic response spectrum and medium sand (ground class C) were used. A behaviour factor of four was selected, corresponding to a ductility class medium frame. A PGA of 0.306g was selected for the building site [16].

Planar models and linear-elastic analysis were used to determine the response of the structures according to Eurocode 8 Cl 4.2.3. The 4-storey and 8-storey structures were designed using the lateral force method in accordance with Eurocode 8 Cl 4.3.3.2.3. The 16-storey structure could not be designed using the lateral force method, as it failed the requirement that the fundamental period (T_1) be less than or equal to 2s. Instead, modal response spectrum analysis was performed in SAP2000 [17] to determine the appropriate seismic loads in accordance with Eurocode 8 Cl 4.3.3.3.

Class one braces were used, meeting the requirements of Eurocode 8 Cl 6.5.3 for medium ductility and a behaviour factor of four. This also ensures sufficient local ductility of brace members to reduce susceptibility to low cycle fatigue failures. Only tension diagonals were considered during elastic analysis in accordance with Eurocode 8 Cl 6.7.2. It is known that CBF structures are prone to form soft-storey mechanisms [18–22]. Eurocode 8 Cl 6.7.4 requires that the maximum overstrength (Ω) of an individual brace not differ from the minimum value by more than 25%. The aim is to promote the simultaneous yield of braces at every storey. The design seismic axial forces of columns are amplified to account for brace overstrength (Eurocode 8 Cl 6.7.4) to ensure satisfactory capacity of the non-dissipative members until brace yield.

Respecting the brace uniformity condition led to excessive overdesign of braces, confirming the findings of several researchers [19,23,24]. Column continuity along the building height can compensate for relaxing the overstrength continuity requirement [18–20,25]. In order to produce feasible designs, braces on the top two storeys of 8S, 16S and 8D were excluded from the uniformity condition. The selection of many brace sections was still governed by uniformity despite this modification. The design of the advanced drift buildings was governed by deflections.

The structural system is composed of standard UK structural steel sections: UK beam (UKB), UK column (UKC), and structural hollow (SHS) sections. The columns and bracing are sections are Grade S355, with a nominal yield stress of 355 MPa [26]. Appendix A presents the final sections for all building designs.

2.3 OpenSees Modelling

The buildings were then modelled in OpenSees [10]. Members are represented by line beam-column elements spanning between two nodes. Seismic masses due to gravity loads and member self-weight were lumped at nodes. Connections were defined as perfectly pinned or perfectly rigid. Rigid diaphragm constraints in the x direction were imposed on all nodes of

each floor level using rigid truss elements. A leaning column [12,27–29] was employed to account for P-Delta effects from the vertical loads acting on gravity columns in the tributary plan area.

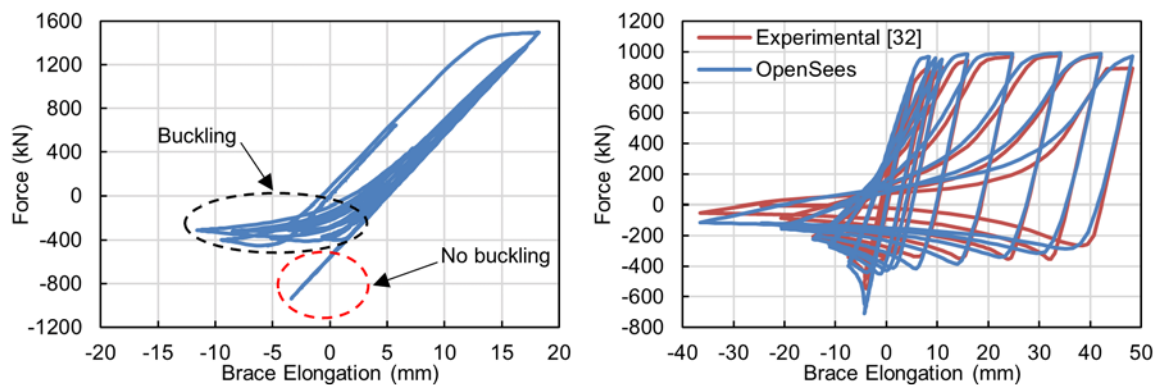
Distributed plasticity force-based beam-column elements were used to model columns with the OpenSees default Gauss-Lobatto integration [30,31]. Five integration points were used for the columns. Based on a parametric study and the recommendations of Kostic and Filippou [31], sections were modelled using 12 fibres for major axis bending and 40 fibres for minor axis bending.

Previous experimental studies [28,32,33] have highlighted the complex nonlinear behaviour of brace members. A wide range of analytical models have been developed, and are discussed in several papers [28,30,34–37]. Uriz *et al.* [30] proposed a physical-theory model that has been used extensively in seismic studies since its introduction [35,36,38–43].

The Uriz method was chosen to model brace members in this paper. Large displacement geometry is accounted for during the transformation from the element reference system to the global reference system using the corotational formulation. The Menegotto-Pinto material is used for the cross-section fibres. At least two elements are used to represent a single brace member, with a node placed at the brace midspan. An initial camber at the brace midpoint is introduced to induce axial buckling. Uriz *et al.* [30] recommended the following model parameters: three integration points, two beam-column elements, an initial camber of 0.05% to 0.1% of the brace length, and ten to 15 fibre layers across the cross-section depth with five layers in the tension and compression edges.

Five fibre layers across the depth of each flange and five fibre layers along the web were used for the SHS brace section. Two layers were used in the widths. The Menegotto-Pinto material is used with a yield stress of 355 MPa. The strain-hardening ratio was set to 0.3% [28].

There has been a wide variety of proposals for the number of elements and the corresponding number of integration points for a brace member [36,40–42]. In the present study, each brace was modelled using two elements and three integration points, as hysteretic behaviour was relatively insensitive to these parameters. External studies [35,42] observed that the initial buckling load is affected by the imperfection value, however the effect is insignificant on the hysteretic area, buckling loads at subsequent cycles, and overall post-buckling response. Only accuracy in the total dissipated energy is required in this study. An initial imperfection of 0.1% at the midspan was selected. It was discovered that the brace imperfection could straighten following tension loading. Buckling would not occur once the camber was numerically zero (see Figure 3a). To ensure the possibility of brace buckling, a fictitious force was applied at the midspan that developed 5% of the yield moment as described by Uriz [28]. The final analytical model to be used in this project was verified using cyclic loading experimental data from Black *et al.* [32], shown in Figure 3b.



(a) Example of compression error without fictitious force (b) Validation of brace model with experimental data
Figure 3: Brace modeling in OpenSees

Inherent damping of 5% was modelled using mass and tangent stiffness proportional Rayleigh damping. Tangent stiffness is more appropriate than initial stiffness for CBFs [36,44,45]. The first and third modes were used to determine the Rayleigh damping coefficients [46]. The first periods were elongated to prevent the generation of artificial damping as recommended by Charney [44]. Table 1 and Table 2 provide the periods and modal mass participation factors of the buildings, respectively.

Table 1: Periods of buildings

Mode	4S	8S	16S	4D	8D
1	0.52s	0.97s	2.34s	0.37s	0.67s
2	0.20s	0.32s	0.67s	0.14s	0.22s
3	0.12s	0.18s	0.35s	0.09s	0.12s

Table 2: Modal mass participation factors

Mode	4S	8S	16S	4D	8D
1	80.7%	75.0%	65.2%	80.7%	74.2%
2	14.8%	17.4%	21.2%	14.8%	18.1%
3	3.2%	4.2%	6.3%	3.1%	4.5%

2.4 Ground Motion Suites

Suites of ground motion records were compiled to represent the ULS and the SLS earthquake intensities. Records were obtained from the PEER ground motion database [47] using the Eurocode 8 response spectrum. A factor of 0.5 was used to define the SLS spectrum. A maximum of one record was selected per historical earthquake. A linear scale factor was applied to each examined record to minimize the mean squared error (MSE) between the ground motion spectrum and the target Eurocode spectrum over the period range of $0.2T_1$ and $2T_1$ [47]. The scale factor was restricted to a maximum of two to prevent excessively large ground motion scaling, while allowing for enough records to be selected. For each building, 25 ground motions with the smallest MSE were selected for each limit state. This resulted in 50 records per building. Appendix B lists the ground motion properties for all 250 records. The ULS and SLS spectra for the 4-storey standard structure are shown in Figure 4.

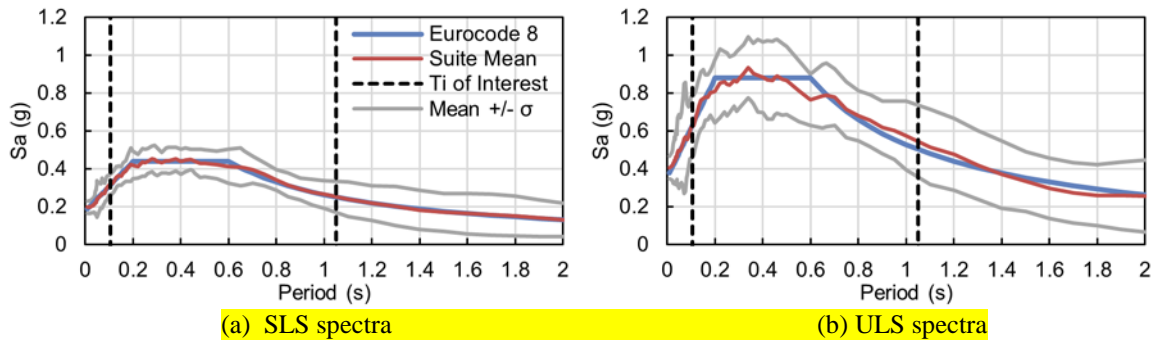


Figure 4: Comparison of the 4S ground motion suite spectra and the Eurocode 8 spectra

2.5 FEMA P-58 Seismic Performance Assessment Procedure

The FEMA P-58 performance assessment procedure [11] was used to evaluate the buildings. FEMA P-58 enables the seismic performance of a structure to be measured in repair costs rather than a set of structural parameters. Each building component at risk during an earthquake is associated with fragility and repair cost functions. Fragility functions indicate the probability of exceeding a damage state at a given value of engineering demand

parameter (EDP). Peak structural response parameters from earthquake analyses are used in combination with fragility functions to determine probable damage states for building components. Repair cost functions then estimate the economic losses for each damage state.

Structural fragility groups and quantities were assigned based on the structural design. Nonstructural fragility groups and quantities were obtained using the median commercial office building quantities from the Normative Quantity Estimation Tool [11]. A seismic design category of D was selected. This represents stringent seismic considerations and is grouped together with D, E and F (essential facilities) within FEMA P-58. Robust equipment anchorage was assumed for HVAC components. These conservative assumptions represent buildings with stringent seismic design and will avoid overestimating repair costs.

2.5.1 Modification of FEMA P-58

The FEMA P-58 documentation recognizes that the CBF fragility functions are strongly influenced by brace detailing and frame design, and must be used with caution [48]. Cutfield *et al.* [43] modified the brace fragility functions, as CBF costs were generated during minor loading when models did not exhibit damage. There are three fragility functions for CBFs in FEMA P-58. CBF damage state one is for aesthetic concerns and repairs are optional; the Consequence Estimation Tool [11] details that approximately 85% of the cost results from temporary access to the member rather than the aesthetic member repair itself.

To assess the significance of this potential source of error, pushover analyses of single CBFs were performed in OpenSees. Each CBF was pushed to an interstorey drift beyond the median drift value for damage state one. It was found that braces behaved in a linear elastic manner with no residual forces or deformations. It was therefore decided to modify the brace fragility functions by removing the fragility function representing damage state one.

Table 3 provides a summary of the critical fragility information used in the project.

Peak floor acceleration (PFA) and interstorey drift ratio (IDR) are EDPs, x_m is the median

EDP value for the damage state, and β is the standard deviation of the natural logarithms of the EDP values.

Table 3: Summary of critical structural and nonstructural system fragility information

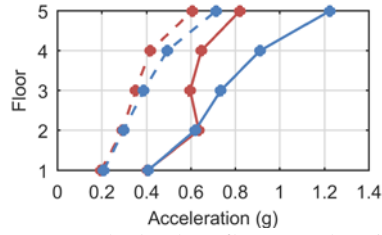
System	EDP	Damage State	x_m	β
Concentric Braced Frame	IDR	Brace buckling and yielding	0.01	0.3
		Brace fracture or local buckling	0.0178	0.3
Glass Curtain Wall	IDR	Glass cracking	0.01097	0.45
		Glass falls from frame	0.01254	0.45
Gypsum wall partition with metal studs	IDR	Minor cracking	0.0021	0.6
		Moderate cracking or crushing	0.0071	0.45
		Significant cracking or crushing	0.012	0.45
Suspended Ceiling, vertical and lateral support	PFA	Minor tiles dislodgement	0.35	0.4
		Moderate tile dislodgement and grid damage	0.55	0.4
		Total ceiling collapse	0.8	0.4
Air Handling Unit	PFA	Equipment does not function	0.25	0.4
Desktop Electronics	PFA	Falls, does not function	0.4	0.5

The replacement cost for desktop electronics was assumed to be \$1800 per unit based on Cutfield *et al.* [43]. The unit costs for work stations, bookcases and filing cabinets were selected as the mean costs from the 2011 National Office Furniture price list [49]. Work stations were set to \$105 per unit (5% of purchase cost as recommended by FEMA P-58), bookcases to \$1350 per unit, and filing cabinets to \$2375 per unit.

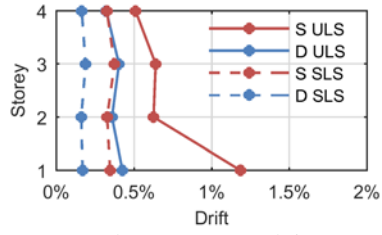
3 Nonlinear Time History Analysis Results

3.1 Engineering Demand Parameters

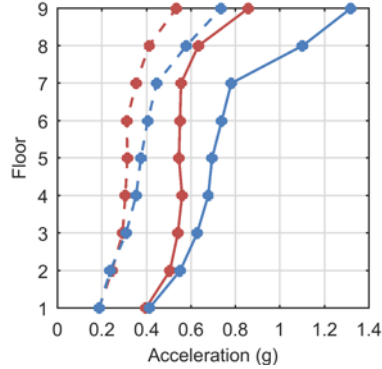
The EDPs used to characterize demands on structural and nonstructural systems in FEMA P-58 are absolute floor acceleration, absolute floor velocity, and interstorey drift. The acceleration and drift results are shown in Figure 5. The mean of the peak EDPs obtained from the 25 time history analyses for each limit state are provided. A range of plus/minus one standard deviation is shown for the 16-storey building but omitted from the 4-storey and 8-storey building graphs for the sake of clarity. The standard deviations of the 4-storey and 8-storey EDPs are smaller than for the 16-storey results. Peak floor velocity results are excluded as the mean values show only modest variation over the building height, with a ULS mean of 4.2 m/s and a SLS mean of 2.5 m/s.



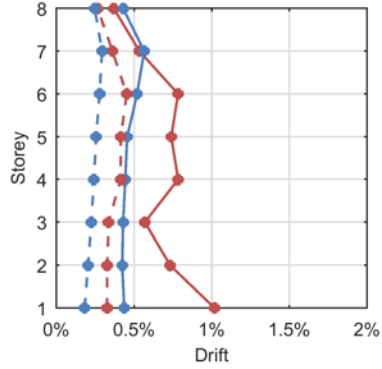
(a) 4-storey peak absolute floor accelerations



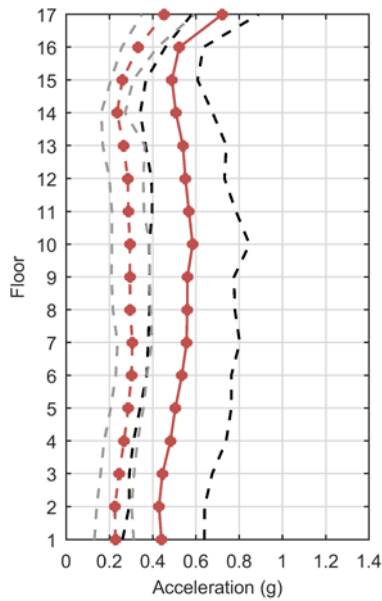
(b) 4-storey peak interstorey drifts



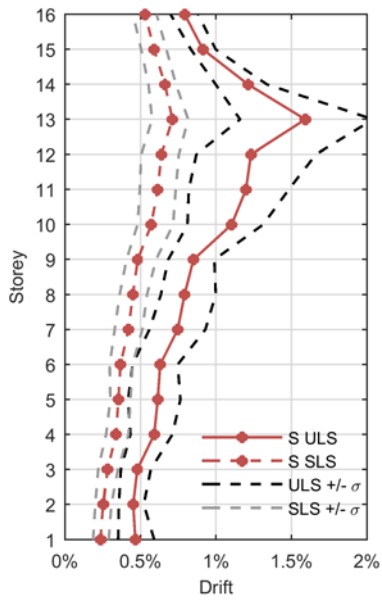
(c) 8-storey peak absolute floor accelerations



(d) 8-storey peak interstorey drifts



(e) 16-storey peak absolute floor accelerations



(f) 16-storey peak interstorey drifts

Figure 5: Mean peak structural response parameters of all buildings from the nonlinear time history analyses

The Eurocode 0.5% drift limit was generally met, predicting ULS serviceability for 4D and 8D, and SLS serviceability for 4S and 8S. Structure 16S exceeds this drift limit in the upper stories. An important result is that the drifts do not exceed 2-3%, the approximate magnitude for the development of a localized plastic collapse mechanism [21].

1 The ULS EDP results have a greater spread than the SLS results, influenced by the
2 variance of the ground motion suites. The ULS suites have a greater average MSE than the
3 SLS suites. The spread of the results also coincides with the significant nonlinear behavior
4 exhibited by the braces during the larger intensity ULS earthquakes. Braces exhibit
5 predominantly elastic behaviour during the SLS with considerable buckling and yielding
6 during the ULS.

7 The standard designs exhibit an uneven distribution of drift demands during the ULS.
8 A concentration of drift occurs in the first storey for 4S. This also occurs for 8S, although in a
9 less pronounced manner. Storey 13 of 16S undergoes significant drift compared to the other
10 storeys. This suggests that the standard buildings have poorly distributed energy dissipation.
11 In comparison, the drift designs avoid the concentration of drifts in individual storeys.

12 The drift designs have a greater maximum acceleration and a lower maximum drift in
13 comparison to the standard designs. The greater accelerations can be attributed to two factors:
14 (1) the drift designs are stiffer (2) it is expected that more nonlinear brace behaviour, and
15 therefore greater energy dissipation through hysteresis, occurs in the standard designs.

16 **3.2 Nonlinear behaviour**

17 The nonlinear brace response of interest can be classified as buckling or yielding.

18 Brace yielding and buckling was determined by examining the force-elongation relationship
19 for each member during each ground motion analysis. Negligible yielding occurs during the
20 SLS for all buildings. The drift designs do not experience buckling during the SLS, while a
21 small number of braces (<6%) buckle in the 4-storey and 8-storey standard buildings. An
22 average of 14% of the braces buckle for the 16-storey standard building. A considerable
23 number of braces yield and buckle during the ULS for the standard buildings. The drift
24 designs experience reduced ULS brace buckling (7% to 17%) due to large brace overstrength
25 resulting from drifts controlling member design. A visualisation of the mean percentage of
26 SLS and ULS analyses per storey that cause brace buckling is provided in Figure 6 for the 4-

storey buildings. Locations of yielding and buckling correlate with the concentration of drifts observed in Figure 5.

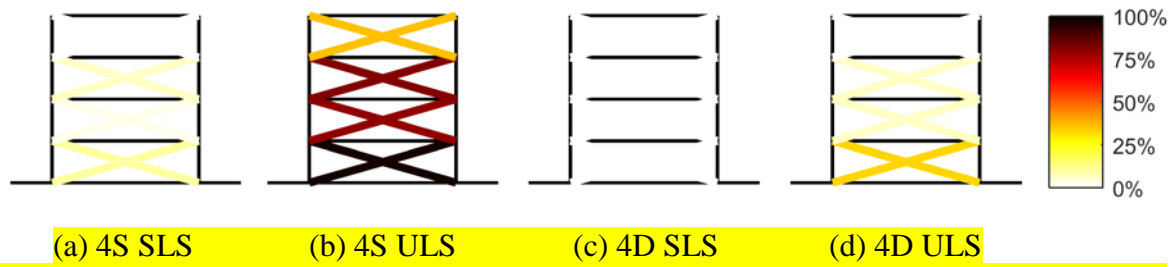


Figure 6: Mean percentage of analyses per storey that cause brace buckling for the 4-storey buildings

Members in non-dissipative zones should withstand the design seismic loading and permit dissipation of seismic energy in the braces [9]. Eight occurrences of column buckling in axial loading-bending were calculated during ULS analyses of the standard buildings. The overcapacity ranged from 1.06 to 1.14. The Eurocode column design procedure produces dominant axial forces in the columns due to brace truss action. Once braces in a storey lose lateral loading capacity due to simultaneous yielding and buckling, continuous columns experience bending. This internal bending due to brace deterioration is not considered in Eurocode design and can lead to under-design of column members.

4 Estimation of Building Value

Estimates of the total building value are needed to give context to the repair costs calculated using FEMA P-58. The RSMeans square foot cost estimator [50] was used to determine building values including material costs, labour costs and contractor fees. San Diego was selected to produce the building cost estimates. Although RSMeans does not include a premium cost option due to seismic design, the selection of a region with substantial seismic risk should incorporate seismic design costs. The RSMeans values are \$3.8M for the 4-storey buildings, \$8.6M for the 8-storey buildings and \$18.2M for the 16-storey building.

Guerrero *et al.* [51] used structural steel weight to interpolate building cost. Structural cost (C_s) is estimated as \$3/kg. It is assumed that the structural system accounts for 20% of the total cost (C_t), i.e. $C_t = 5C_s$. This approach was used to verify the RSMeans estimates.

The estimated costs using the steel weight approach are comparable to the RSMeans costs, with differences between 3% to 14%. The difference in building cost between the standard and advanced drift designs was accounted for using the steel weight approach. The cost increase for the drift designs due to the difference in C_s are \$70,000 for 4D and \$440,000 for 8D. The standard building values were taken as the RSMeans costs. No conversion was made for 2011 dollar values. The final building values are provided in Table 4.

Table 4: Estimated Building Values

Building	Building Value
4S	\$3.8M
8S	\$8.6M
16S	\$18.2M
4D	\$3.87M
8D	\$9.04M

5 Seismic Performance Assessment Results

This section presents the results of the performance assessments carried out using the FEMA P-58 method, expressed as repair costs in 2011 US dollars. Indirect costs due to building downtime are out of scope.

5.1 Total Repair Costs

A Monte Carlo analysis with 1000 realizations for each limit state was conducted, surpassing the minimum number of 500 realizations recommended by the FEMA P-58 methodology [52]. Cumulative distribution functions of the ULS and the SLS total repair costs normalized by the respective building cost are shown in Figure 7. The mean, median and 90th percentile total repair costs are given in Table 5 to provide the non-normalized data. The spread of the ULS data is greater, reflecting the results of the time history analyses.

The SLS cost distributions are comparable amongst all buildings. The median damage ranges from 20% to 23% of the building cost. The SLS repair costs are of concern, as damage at this intensity should be limited to a level which does not compromise building serviceability [9]. The assessment results indicate that extensive repairs are required. It is probable that these repairs will disrupt building function for an extended period. This

suggests that modern building standards do not accomplish earthquake resilience: the ability to quickly recover after an earthquake. The median ULS repairs are approximately 41% to 52% of the building cost. Owners often elect to demolish and replace the existing building if repair costs exceed 40% of the building cost [11]. The ULS results therefore suggest it is probable that many buildings designed to current structural codes may be demolished and replaced following a ULS earthquake.

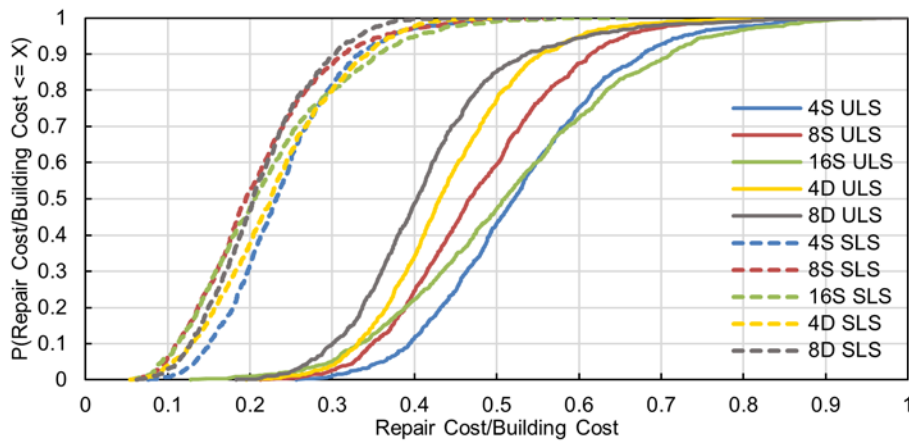


Figure 7: Cumulative distribution functions of the ULS and the SLS total repair costs normalized by building value

Table 5: Total repair costs (\$M) for the ULS and the SLS

Limit State	Building	Mean	Median	90th Percentile
ULS	4S	2.01	1.98	2.58
	8S	4.17	4.13	5.39
	16S	9.40	9.28	12.95
	4D	1.70	1.67	2.14
	8D	3.75	3.65	4.88
SLS	4S	0.91	0.88	1.26
	8S	1.81	1.70	2.71
	16S	4.03	3.75	6.46
	4D	0.89	0.87	1.33
	8D	1.90	1.84	2.73

A comparison of the drift and standard design repair costs is shown in Figure 8. The ULS repair costs of the drift designs are reduced with respect to the standard designs. The median values differ by \$320,000 (16%) for the 4-storey structures and \$480,000 (12%) for the 8-storey structures. In contrast to the ULS results, the SLS repair costs of the drift designs

are not improved. Although the ULS repair costs of the drift designs are reduced, the median repairs still exceed 40% of the building value.

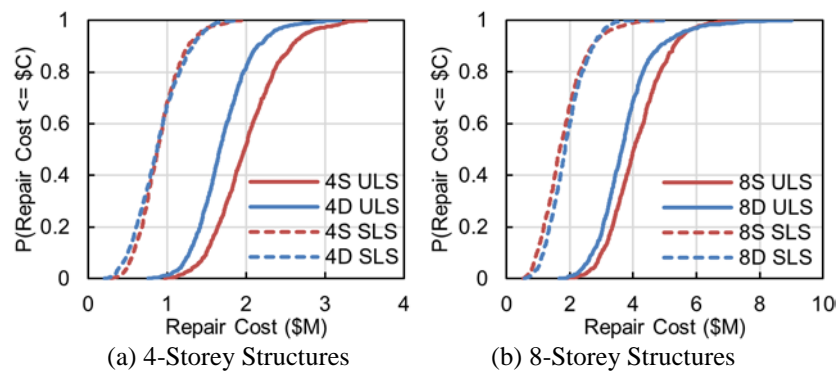


Figure 8: Comparison of the standard and drift design total repair costs expressed as cumulative distribution functions

5.2 Relationship between Repair Costs and EDPs

Mean repair costs related to each EDP are shown in Figure 9, in which the costs have been normalized by the total repair cost of the respective building.

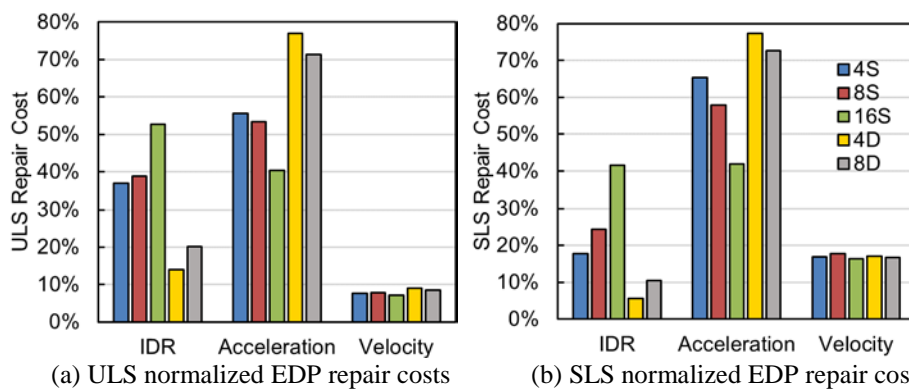


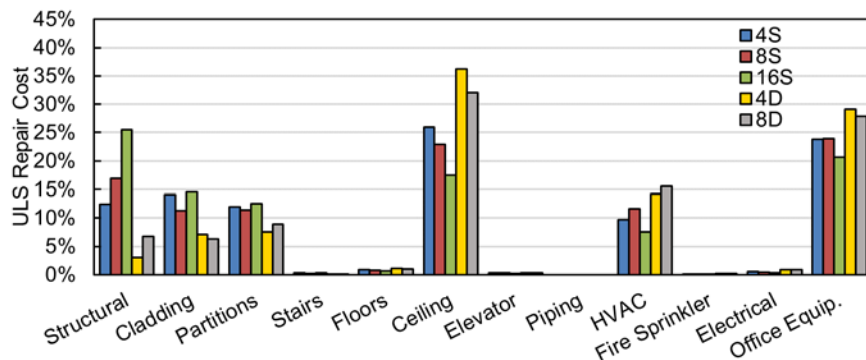
Figure 9: Mean repair costs grouped by associated EDP and normalized by total repair costs

Conventional building codes control drifts but do not place limitations on allowable floor accelerations. Accelerations are only considered for calculations of anchorage strength in the Eurocode. Figure 9 reveals that acceleration-sensitive damage and drift-sensitive damage comprise the majority of repair costs for both limit states. ULS acceleration-sensitive damage is comparable to drift-sensitive damage for building 16S. 16S is the most flexible of the studied buildings and experiences larger drifts. Acceleration damage is responsible for more than half of the 4-storey and 8-storey ULS repair costs. The contribution of acceleration-sensitive damage is even greater for the SLS. This explains why the advanced

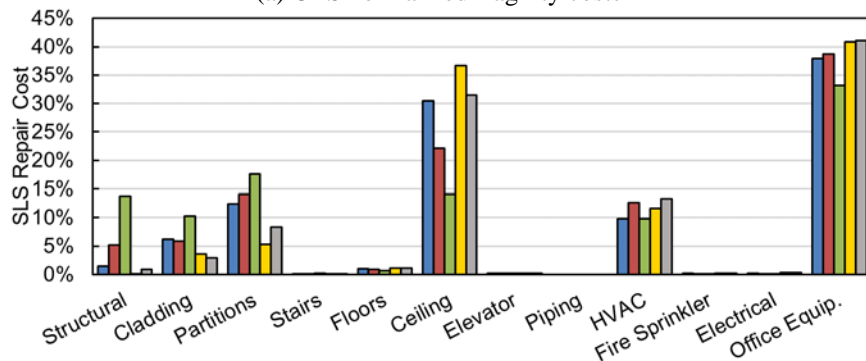
drift designs (buildings 4D and 8D) achieve only modest reductions in total repair costs. The influence of acceleration on seismic performance should be more appropriately reflected in the design procedures of structures.

5.3 Fragility Group Repair Costs

The repair cost of each fragility group is a function of the number of components in the group, the replacement cost per component, and the damage state experienced by each component. The mean repair costs were arranged by the structural and nonstructural fragility groups responsible for the costs. This disaggregation, normalized by the total repair cost for the building, is shown in Figure 10. Negligible repair costs can be attributed to stairs, access flooring, elevators, piping, fire sprinkler systems, and electrical systems. Additional seismic performance studies can exclude these fragility groups with negligible repair costs in order to decrease the required computation time.



(a) ULS normalized fragility costs



(b) SLS normalized fragility costs

Figure 10: Fragility-sorted mean repair costs normalized by total repair costs

Considering the distribution of ULS repair costs, ceilings and office equipment (acceleration-sensitive components) are responsible for the most damage in the 4-storey and

8-storey buildings. The 16-storey building has large repair costs in those fragility groups, however the largest contributor is structural damage. The distribution of fragility group SLS costs remains similar to the ULS distribution with the exception of structural damage. Structural costs significantly decrease to less than 5% of the total costs for the 4-storey and 8-storey buildings. The 16-storey structure does not adhere to this outcome as the structural damage is approximately 15% of the total costs.

Brace damage is responsible for the majority of the structural cost. Structural damage is anticipated for the ULS, as conventional seismic design relies on structural members experiencing inelastic deformation. These large inelastic deformations are concentrated in members designed to dissipate seismic energy in a controlled manner. Structural damage would introduce significant delays to building re-occupancy and should be minimised during the SLS. Based on Figure 10, structural damage would delay building re-occupancy following an SLS event for 8S and 16S. The level of structural damage is successfully reduced by the drift designs.

The previous section found that the median ULS repair costs of the drift designs exceed the 40% building value limit that often triggers a decision to replace the building. Figure 10 reveals that building 4D sustains only minimal structural damage during the ULS. This reveals that the 40% replacement level is not a strict guideline, as it is unlikely that building 4D would be demolished without sustaining notable structural damage.

Nonstructural systems are treated in a simplified manner during structural design. Between 74% to 88% of the ULS costs and between 86% and 99% of the SLS costs of the standard buildings can be attributed to these systems. This demonstrates the importance of considering nonstructural seismic performance when designing for a rapid return to building occupancy. Attaining a target level of seismic performance mandates the harmonization of structural and nonstructural performance levels.

6 Effectiveness of Eurocode 8 Drift Limits

The FEMA P-58 analyses in this paper revealed that Eurocode compliant structures exhibit poor nonstructural seismic performance. According to the Eurocode provisions, nonstructural damage should be minimised at the storeys satisfying the 0.5% drift limit. However, storeys with mean drifts well under the allowable limit still experienced nonstructural damage. These results suggest that the Eurocode drift limit is inadequate to prevent damage to drift-sensitive nonstructural systems. Acceleration-sensitive nonstructural systems also produce extensive repair costs, and this EDP is not controlled by the drift requirement. It should be noted that the studied nonstructural systems are of the highest seismic design category. A significant increase in nonstructural repair costs would be expected for buildings with more vulnerable systems. These results highlight the need for further review of the Eurocode nonstructural provisions.

7 FEMA P-58 Repair Costs Sensitivity Study

The sensitivity of FEMA P-58 repair cost calculations to the use of initial or tangent stiffness Rayleigh damping, the assumed nonstructural quantities, and the assumed nonstructural seismic design category was investigated.

7.1 Rayleigh Damping

The effect of using initial or tangent stiffness proportional Rayleigh damping on the calculation of repair costs was examined. Figure 11 illustrates the magnitude of the difference in repair costs. Repair cost distributions for the largest difference (4S) and the second largest difference (16S) are provided. Across all the structures, it was found that repair costs are reduced by between 1% and 7% when using initial stiffness. The drift designs and the SLS results are less sensitive to the use of initial or tangent stiffness, as would be expected, since in these cases the structures remain elastic for larger portions of the time history analyses.

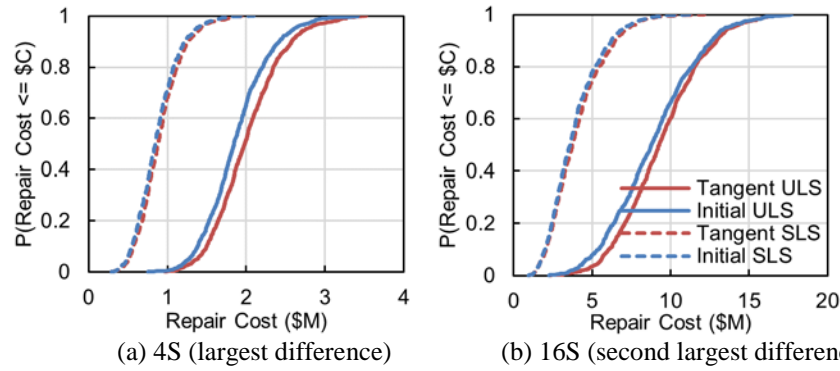


Figure 11: Repair cost distributions considering the use of initial and tangent stiffness proportional Rayleigh damping

7.2 Nonstructural Quantities

The sensitivity of the calculated costs to probable differences in nonstructural component quantities was examined. The 90th percentile of office nonstructural component quantities was chosen to approximate an upper bound on nonstructural damage for buildings that are densely populated. The quantities were obtained using the Normative Quantity Estimation Tool [11]. The resulting change in repair costs was considerable. Costs increased by 17% to 36%. Figure 12 illustrates the influence of nonstructural quantities on the calculated repair costs.

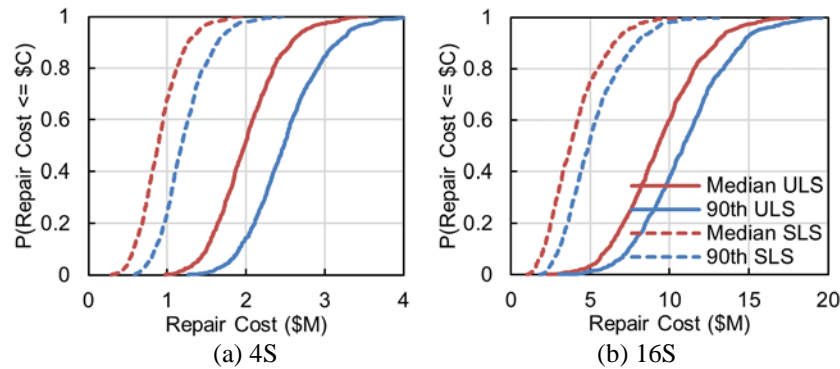


Figure 12: Repair cost distributions considering the use of median and 90th percentile nonstructural quantities

7.3 Nonstructural Specifications

The sensitivity of repair costs to the seismic design category of nonstructural systems was investigated. Seismic design category A/B was selected to represent standard nonstructural components. The sensitivity of the repair costs to the nonstructural quantities was found to be significant. Repair costs increased by 6% to 26%. Figure 13 displays the impact of seismic design category selection on the repair cost distributions. These results demonstrate that

advanced nonstructural specifications such as lateral bracing do improve repair costs. However, the buildings with strict nonstructural specifications still experience extensive nonstructural damage. This suggests that advanced nonstructural detailing alone cannot prevent damage. There is a need and opportunity for building-level solutions such as the use of fluid viscous dampers.

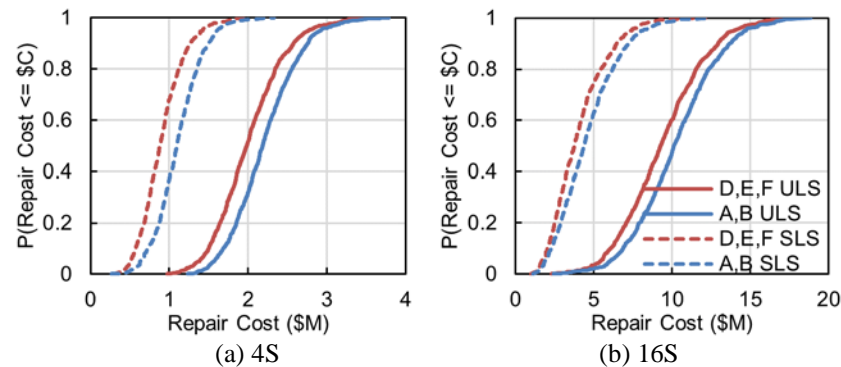


Figure 13: Repair cost distributions considering the use of different nonstructural seismic design categories

8 Conclusions

This paper investigates the seismic performance of conventional multi-storey buildings designed for seismic regions using Eurocode 8. Structural response parameters used to characterize demands on structural and nonstructural systems were determined from nonlinear time history analyses of representative buildings modelled in OpenSees. The Eurocode 0.5% drift limit was generally met: predicting ULS serviceability for 4D and 8D, and SLS serviceability for 4S and 8S. The FEMA P-58 procedure was used to measure seismic performance in repair costs.

Buildings designed to modern structural standards may be demolished following a ULS earthquake due to the high repair costs. Substantial repair costs were calculated for the SLS scenario, including structural damage for 8S and 16S. The direct costs would be compounded by indirect costs due to downtime. These results suggest that modern building standards do not accomplish earthquake resilience: the ability of a community to recover quickly after an earthquake.

1 The level of structural damage was reduced by the drift designs. Although the ULS
2 repair costs decrease, median repairs are still above the 40% building value limit that
3 corresponds to building replacement. However the 40% replacement level is not a strict
4 guideline, as it is unlikely that the 4D structure would be demolished without sustaining
5 notable structural damage. SLS repair costs comparable to the standard designs were realized.

6 Conventional building codes control drifts but do not place limitations on floor
7 accelerations. It was observed that acceleration-sensitive damage is of comparable or greater
8 consequence than drift-sensitive damage. The influence of acceleration on seismic
9 performance should be more appropriately reflected in structural design procedures.

10 Nonstructural systems are treated in a simplified manner during structural design.
11 However, the majority of repair costs can be attributed to these systems. This highlights the
12 importance of considering nonstructural seismic performance when designing for a rapid
13 return to building occupancy. Attaining a target level of seismic performance mandates the
14 harmonization of structural and nonstructural performance.

15 The FEMA P-58 repair cost calculations were found to be sensitive to the quantity
16 and the seismic design category of the nonstructural components.

17 Limitations of the Eurocode damage mitigation methodology were exposed as the
18 prescribed drift limit did not prevent nonstructural damage. Storeys satisfying the limit
19 experienced drift-sensitive nonstructural damage. Extensive acceleration-sensitive
20 nonstructural costs were also produced. It should be noted that the studied nonstructural
21 systems are of the highest seismic design category. Significant amplification of repair costs
22 would be expected for more vulnerable systems. These results draw attention to the need for
23 structural design procedures which enhance nonstructural seismic performance. This shift in
24 seismic design philosophy is required to achieve a rapid return to building occupancy after an
25 earthquake.

Funding

This work was supported by the Clarendon Fund, and the Natural Sciences and Engineering Research Council of Canada [CGS M, PSG D]

References

- [1] Taghavi S, Miranda E. Response assessment of nonstructural building elements. Berkeley, USA: 2003.
- [2] Fierro EA, Miranda E, Perry CL. Behavior of nonstructural components in recent earthquakes. *Archit. Eng. Conf.* 2011, Oakland, California, United States: American Society of Civil Engineers (ASCE); 2011, p. 369–77.
- [3] Dhakal RP. Damage to non-structural components and contents in 2010 Darfield earthquake. *Bull New Zeal Soc Earthq Eng* 2010;43:404–11.
- [4] Miranda E, Mosqueda G, Retamales R, Pekcan G. Performance of nonstructural components during the 27 February 2010 Chile earthquake. *Earthq Spectra* 2012;28:S453–71. doi:10.1193/1.4000032.
- [5] Lavan O, Dargush GF. Multi-Objective Evolutionary Seismic Design with Passive Energy Dissipation Systems. *J Earthq Eng* 2009;13:758–90. doi:10.1080/13632460802598545.
- [6] Terzic V, Mahin SA, Comerio M. Comparative life-cycle cost and performance analysis of structural systems for buildings. 10th US Natl Conf Earthq Eng Front Earthq Eng NCEE 2014 2014. doi:10.4231/D3930NW0G.
- [7] Motahari S a., Ghassemieh M, Abolmaali S a. Implementation of shape memory alloy dampers for passive control of structures subjected to seismic excitations. *J Constr Steel Res* 2007;63:1570–9. doi:10.1016/j.jcsr.2007.02.001.
- [8] Mahjoubi S, Maleki S. Seismic performance assessment of steel frames equipped with a novel passive damper using a new damper performance index. *Struct Control Heal Monit* 2015;22:774–97.
- [9] CEN. Eurocode 8: Design of structures for earthquake resistance - Part 1: General rules, seismic actions and rules for buildings 2013.
- [10] McKenna F. OpenSees 2017.
- [11] FEMA. FEMA P-58, Seismic Performance Assessment of Buildings, Methodology and Implementation. Washington, D.C.: 2012.
- [12] Chen C, Mahin SA. Performance-based seismic demand assessment of concentrically braced steel frame buildings. Berkeley, USA: 2012.
- [13] CEN. Eurocode: Basis of structural design 2010.
- [14] CEN. Eurocode 1: Actions on structures 2010.
- [15] CEN. Eurocode 3: Design of steel structures 2010.
- [16] Solomos G, Pinto A, Dimova S. A review of the seismic hazard zonation in national building codes in the context of Eurocode 8. *JRC Sci Tech Reports* 2008.
- [17] Computers and Structures Inc. SAP2000 2013.
- [18] Tremblay R. Achieving a Stable Inelastic Seismic Response for Multi-Story Concentrically Braced Steel Frames. *Eng J* 2003;40:111–29.
- [19] Elghazouli AY. Assessment of European seismic design procedures for steel framed structures. *Bull Earthq Eng* 2010;8:65–89. doi:10.1007/s10518-009-9125-6.
- [20] Ji X, Kato M, Wang T, Hitaka T, Nakashima M. Effect of gravity columns on mitigation of drift concentration for braced frames. *J Constr Steel Res* 2009;65:2148–56. doi:10.1016/j.jcsr.2009.07.003.
- [21] Merczel DB, Somja H, Aribert J-M, Lógó J. On the behaviour of concentrically braced frames subjected to seismic loading. *Period Polytech Civ Eng* 2013;57:113–22. doi:10.3311/PPci.7167.

- [22] Banihashemi MR, Mirzagoltabar AR, Tavakoli HR. Performance-based plastic design method for steel concentric braced frames. *Int J Adv Struct Eng* 2015;7:281–93.
- [23] Brandonisio G, Toreno M, Grande E, Mele E, De Luca a. Seismic design of concentric braced frames. *J Constr Steel Res* 2012;78:22–37. doi:10.1016/j.jcsr.2012.06.003.
- [24] Merczel DB, Aribert JM, Somja H, Hjiat M. Plastic analysis-based seismic design method to control the weak storey behaviour of concentrically braced steel frames. *J Constr Steel Res* 2016;125:142–63. doi:10.1016/j.jcsr.2016.05.008.
- [25] MacRae GA, Kimura Y, Roeder C. Effect of Column Stiffness on Braced Frame Seismic Behavior. *J Struct Eng* 2004;130:381–91.
- [26] Tata Steel Europe Limited. *Tata Steel Sections Blue Book* 2014.
- [27] Goulet CA, Haselton CB, Mitrani-Reiser J, Beck JL, Deierlein GG, Porter KA, et al. Evaluation of the seismic performance of a code-conforming reinforced-concrete frame building - from seismic hazard to collapse safety and economic losses. *Earthq Eng Struct Dyn* 2007;36:1973–97. doi:10.1002/eqe.
- [28] Uriz P, Mahin S. *Toward earthquake-resistant design of concentrically braced steel-frame structures*. Berkeley, USA: 2008.
- [29] Jarrett J a., Judd JP, Charney F a. Comparative evaluation of innovative and traditional seismic-resisting systems using the FEMA P-58 procedure. *J Constr Steel Res* 2015;105:107–18. doi:10.1016/j.jcsr.2014.10.001.
- [30] Uriz P, Filippou FC, Mahin SA. Model for Cyclic Inelastic Buckling of Steel Braces. *J Struct Eng* 2008;134:619–28. doi:10.1061/(ASCE)0733-9445(2008)134:4(619).
- [31] Kostic SM, Filippou FC. Section Discretization of Fiber Beam-Column Elements for Cyclic Inelastic Response. *J Struct Eng* 2012;138:592–601. doi:10.1061/(ASCE)ST.1943-541X.0000501.
- [32] Black RG, Wenger WA, Popov EP. *Inelastic Buckling of Steel Struts Under Cyclic Load Reversal* 1980:Report No. UCB/EERC-80/40.
- [33] Tremblay R. Inelastic seismic response of steel bracing members. *J Constr Steel Res* 2002;58:665–701. doi:10.1016/S0143-974X(01)00104-3.
- [34] Jin J, El-Tawil S. Inelastic Cyclic Model for Steel Braces. *J Eng Mech* 2003;129:548–57. doi:10.1061/(ASCE)0733-9399(2003)129:5(548).
- [35] Wijesundara KK, Nascimbene R, Rassati G a. Modeling of different bracing configurations in multi-storey concentrically braced frames using a fiber-beam based approach. *J Constr Steel Res* 2014;101:426–36. doi:10.1016/j.jcsr.2014.06.009.
- [36] Karamanci E, Lignos D. Computational Approach for Collapse Assessment of Concentrically Braced Frames in Seismic Regions. *J Struct Eng* 2014;140. doi:10.1061/(ASCE)ST.1943-541X.0001011.
- [37] Hsiao P-C, Lehman DE, Roeder CW. Improved analytical model for special concentrically braced frames. *J Constr Steel Res* 2012;73:80–94. doi:10.1016/j.jcsr.2012.01.010.
- [38] Erduran E, Dao ND, Ryan KL. Comparative response assessment of minimally compliant low-rise conventional and base-isolated steel frames. *Earthq Eng Struct Dyn* 2012;40:1123–41.
- [39] Goggins J, Salawdeh S. Validation of nonlinear time history analysis models for single-storey concentrically braced frames using full-scale shake table tests. *Earthq Eng Struct Dyn* 2013;42:1151–70.
- [40] Salawdeh S, Goggins J. Numerical simulation for steel brace members incorporating a fatigue model. *Eng Struct* 2013;46:332–49. doi:10.1016/j.engstruct.2012.07.036.
- [41] McCrum DP, Broderick BM. An experimental and numerical investigation into the seismic performance of a multi-storey concentrically braced plan irregular structure.

- 1 Bull Earthq Eng 2013;11:2363–85. doi:10.1007/s10518-013-9470-3.
- 2 [42] D’Aniello M, La Manna Ambrosino G, Portioli F, Landolfo R. The influence of out-
3 of-straightness imperfection in physical theory models of bracing members on seismic
4 performance assessment of concentric braced structures. Struct Des Tall Spec Build
5 2015;24:176–97.
- 6 [43] Cutfield M, Ryan K. Comparative Life Cycle Analysis of Conventional and Base
7 Isolated Buildings. Earthq Spectra 2016;32:323–43.
- 8 [44] Charney FA. Unintended consequences of modeling damping in structures. J Struct
9 Eng 2008;134:581–92.
- 10 [45] D’Aniello M, La Manna Ambrosino G, Portioli F, Landolfo R. Modelling aspects of
11 the seismic response of steel concentric braced frames. Steel Compos Struct
12 2013;15:539–66. doi:10.12989/scs.2013.15.5.539.
- 13 [46] Chopra AK. Dynamics of Structures. 4th ed. New Jersey: Prentice Hall; 2012.
- 14 [47] PEER. PEER NGA-WEST 2 Ground Motion Database 2013.
15 <http://ngawest2.berkeley.edu/site>.
- 16 [48] Roeder CW, Lehman DE, Lumpkin E. Fragility Curves for Concentrically Braced
17 Steel Frames with Buckling Braces. 2009.
- 18 [49] National Office Furniture. National Office Furniture - Casegoods 2011.
- 19 [50] RSMeans Online. Square Foot Estimator 2017. www.rsmeansonline.com (accessed
20 April 10, 2017).
- 21 [51] Guerrero H, Terán-Gilmore A, Ji T, Escobar JA. Evaluation of the economic benefits
22 of using Buckling-Restrained Braces in hospital structures located in very soft soils.
23 Eng Struct 2017;136:406–19. doi:10.1016/j.engstruct.2017.01.038.
- 24 [52] FEMA. FEMA P-58, Seismic Performance Assessment of Buildings, Volume 2 -
25 Implementation Guide. vol. 2. Washington, D.C.: 2012.
- 26
- 27

Appendix A: Structural Sections

The brace and column sections are provided in Table A1 – A5. The brace overstrength factors are also provided. Interior columns refers to the inner gravity columns and exterior columns refers to the perimeter columns. Only the smaller section size is provided in the tables for the storeys in which a column section change occurs.

Table A1: Column and brace information of building 4S

Storey	Column (UKC)		Brace(SHS)	Ω
	Interior	Exterior		
4	203x203x71	254x254x167	140x140x5	1.42
3	203x203x71	254x254x167	140x140x8	1.18
2	203x203x71	254x254x167	140x140x12.5	1.22
1	203x203x71	254x254x167	140x140x12.5	1.11

Table A2: Column and brace information of building 8S

Storey	Column (UKC)			Brace(SHS)	Ω
	Interior	Exterior	Corner		
8	152x152x44	152x152x51	203x203x71	140x140x5	4.08
7	152x152x44	152x152x51	203x203x71	140x140x5	1.8
6	203x203x71	203x203x100	254x254x132	140x140x5	1.24
5	203x203x71	203x203x100	254x254x132	140x140x6.3	1.18
4	203x203x113	254x254x167	305x305x198	140x140x6.3	1.05
3	203x203x113	254x254x167	305x305x198	140x140x8	1.13
2	254x254x132	305x305x240	305x305x283	140x140x8	1.09
1	254x254x132	305x305x240	305x305x283	140x140x8	1.04

Table A3: Column and brace information of building 16S

Storey	Column (UKC)			Brace(SHS)	Ω
	Interior	Exterior	Corner		
16	152x152x44	203x203x71	203x203x71	140x140x5	4.39
15	152x152x44	203x203x71	203x203x71	140x140x5	2.36
14	203x203x71	203x203x100	203x203x100	140x140x5	1.76
13	203x203x71	203x203x100	203x203x100	140x140x5	1.54
12	203x203x100	254x254x132	254x254x167	140x140x6.3	1.66
11	203x203x100	254x254x132	254x254x167	140x140x6.3	1.55
10	254x254x132	305x305x198	305x305x198	140x140x6.3	1.47
9	254x254x132	305x305x198	305x305x198	140x140x8	1.64
8	254x254x167	305x305x240	305x305x240	140x140x8	1.56
7	254x254x167	305x305x240	305x305x240	140x140x8	1.5
6	305x305x198	305x305x283	356x406x287	140x140x10	1.64
5	305x305x198	305x305x283	356x406x287	140x140x10	1.58
4	305x305x198	305x406x340	356x406x393	140x140x10	1.53
3	305x305x198	305x406x340	356x406x393	140x140x12.5	1.68
2	305x305x240	356x406x393	356x406x467	140x140x12.5	1.66
1	305x305x240	356x406x393	356x406x467	140x140x12.5	1.57

Table A4: Column and brace information of building 4D

Storey	Column (UKC)			Brace(SHS)	Ω
	Interior	Exterior	Corner		
4	203x203x71	254x254x167	305x305x198	140x140x5	2.49
3	203x203x71	254x254x167	305x305x198	140x140x8	2.02
2	203x203x71	254x254x167	305x305x198	140x140x12.5	2.13
1	203x203x71	254x254x167	305x305x198	140x140x12.5	1.93

Table A5: Column and brace information of building 8D

Storey	Column (UKC)			Brace(SHS)	Ω
	Interior	Exterior	Corner		
8	152x152x44	203x203x60	203x203x100	140x140x12.5	7.39
7	152x152x44	203x203x60	203x203x100	140x140x12.5	3.3
6	203x203x71	254x254x167	305x305x198	160x160x14.2	2.86
5	203x203x71	254x254x167	305x305x198	180x180x14.2	2.59
4	203x203x113	305x305x283	356x406x340	180x180x14.2	2.46
3	203x203x113	305x305x283	356x406x340	180x180x14.2	2.46
2	254x254x132	356x406x393	356x406x551	180x180x14.2	2.35
1	254x254x132	356x406x393	356x406x551	180x180x14.2	2.23

Appendix B: Ground Motion Suites

Records were obtained from the PEER ground motion database [47]. Table B.1 –

B.10 provide the ground motion suites used in the performance assessments for each building. RSN refers to the record sequence number of the ground motion, Mag. refers to the magnitude of the ground motion, scale refers to the linear scale factor applied to the ground motion, and MSE is the mean squared error of the ground motion spectrum with respect to the Eurocode 8 spectrum.

1

Table B1: 4S ULS ground motion suite

Earthquake	Station	RSN	Mag.	Scale	MSE
Imperial Valley-02, 1940	El Centro Array #9	6	6.95	1.2069	0.0255
Managua Nicaragua-01, 1972	Managua ESSO	95	6.24	1.1149	0.0645
Gazli USSR, 1976	Karakyr	126	6.8	0.6893	0.05
Imperial Valley-06, 1979	Delta	169	6.53	1.4044	0.0278
Westmorland, 1981	Westmorland Fire Sta	319	5.9	0.9871	0.0519
Coalinga-01, 1983	Cantua Creek School	322	6.36	1.622	0.0369
Chalfant Valley-02, 1986	Zack Brothers Ranch	558	6.19	0.7751	0.0404
Whittier Narrows-01, 1987	Compton - Castlegate St	611	5.99	1.2323	0.0161
Superstition Hills-02, 1987	El Centro Imp. Co. Cent	721	6.54	1.2138	0.0415
Loma Prieta, 1989	Palo Alto - 1900 Embarc.	786	6.93	1.4673	0.0427
Erzican Turkey, 1992	Erzincan	821	6.69	1.0932	0.0459
Big Bear-01, 1992	Desert Hot Springs	902	6.46	1.7779	0.0451
Northridge-01, 1994	Arleta - Nordhoff Fire Sta	949	6.69	1.1602	0.033
Kobe Japan, 1995	Shin-Osaka	1116	6.9	1.5623	0.0552
Dinar Turkey, 1995	Dinar	1141	6.4	1.1007	0.0701
Kocaeli Turkey, 1999	Duzce	1158	7.51	1.2637	0.0397
Chi-Chi Taiwan, 1999	TCU055	1495	7.62	1.4795	0.0574
Chi-Chi Taiwan-03, 1999	TCU065	2618	6.2	1.8828	0.0787
Parkfield-02 CA, 2004	PARKFIELD - UPSAR 10	4146	6	1.5421	0.0337
Friuli (aftershock 9) Italy, 1976	Buia	4276	5.5	1.8704	0.0502
Chuetsu-oki Japan, 2007	NIG018	5264	6.8	0.7829	0.0193
Iwate Japan, 2008	Nakashinden Town	5774	6.9	1.8091	0.0447
El Mayor-Cucapah Mexico, 2010	Chihuahua	5823	7.2	1.5505	0.0265
Darfield New Zealand, 2010	Kaiapoi North School	6923	7	1.2294	0.0253
Christchurch New Zealand, 2011	Christchurch Botanical Gardens	8063	6.2	0.8172	0.0294

2

3

Table B2: 4S SLS ground motion suite

Earthquake	Station	RSN	Mag.	Scale	MSE
Imperial Valley-02, 1940	El Centro Array #9	6	6.95	0.6069	0.0255
Northern Calif-03, 1954	Ferndale City Hall	20	6.5	1.1649	0.0329
Point Mugu, 1973	Port Hueneme	97	5.65	1.8583	0.0315
Imperial Valley-06, 1979	Delta	169	6.53	0.7062	0.0278
Victoria Mexico, 1980	Chihuahua	266	6.33	1.2	0.0305
Coalinga-01, 1983	Cantua Creek School	322	6.36	0.8156	0.0369
Morgan Hill, 1984	Halls Valley	461	6.19	1.0438	0.0356
Taiwan SMART1(45), 1986	SMART1 O08	582	7.3	1.3726	0.0341
Whittier Narrows-01, 1987	Compton - Castlegate St	611	5.99	0.6197	0.0161
Loma Prieta, 1989	Fremont - Emerson Court	761	6.93	1.3331	0.0138
Northridge-01, 1994	Manhattan Beach - Manhattan	1035	6.69	1.2179	0.0188
Kobe Japan, 1995	Sakai	1115	6.9	1.1217	0.0379
Kocaeli Turkey, 1999	Zeytinburnu	1177	7.51	1.9258	0.0293
Chi-Chi Taiwan, 1999	TCU098	1526	7.62	1.5554	0.0125
Manjil Iran, 1990	Abhar	1634	7.37	1.2154	0.0345
Northridge-06, 1994	Sylmar - Converter Sta	1736	5.28	1.036	0.036
Chi-Chi Taiwan-03, 1999	CHY101	2507	6.2	1.5489	0.0376
Whittier Narrows-02, 1987	Bell Gardens - Jaboneria	3687	5.27	1.7242	0.0379
Chi-Chi Taiwan-06, 1999	CHY004	3864	6.3	1.9193	0.0275
Parkfield-02 CA, 2004	Parkfield - Fault Zone 15	4117	6	1.255	0.0275
Niigata Japan, 2004	FKS028	4159	6.63	1.4788	0.0386
Chuetsu-oki Japan, 2007	Hinodecho Yoshida Tsubame City	4880	6.8	1.489	0.0361
El Mayor-Cucapah Mexico, 2010	Chihuahua	5823	7.2	0.7797	0.0265
Darfield New Zealand, 2010	Kaiapoi North School	6923	7	0.6182	0.0253
Christchurch New Zealand, 2011	LINC	8102	6.2	1.791	0.0309

4

1

Table B3: 8S ULS ground motion suite

Earthquake	Station	RSN	Mag.	Scale	MSE
Imperial Valley-02, 1940	El Centro Array #9	6	6.95	1.3217	0.0312
Managua Nicaragua-01, 1972	Managua ESSO	95	6.24	1.3233	0.0844
Gazli USSR, 1976	Karakyr	126	6.8	0.7409	0.0344
Imperial Valley-06, 1979	Delta	169	6.53	1.5527	0.0331
Westmorland, 1981	Westmorland Fire Sta	319	5.9	0.994	0.0535
Coalinga-01, 1983	Pleasant Valley P.P. - bldg	367	6.36	1.1072	0.0444
N. Palm Springs, 1986	North Palm Springs	529	6.06	0.8586	0.0567
Chalfant Valley-02, 1986	Zack Brothers Ranch	558	6.19	0.8604	0.0784
Superstition Hills-02, 1987	El Centro Imp. Co. Cent	721	6.54	1.2911	0.0264
Loma Prieta, 1989	Hollister Differential Array	778	6.93	1.341	0.0533
Big Bear-01, 1992	Desert Hot Springs	902	6.46	1.9301	0.0902
Northridge-01, 1994	LA - Hollywood Stor FF	995	6.69	1.8409	0.0353
Kobe Japan, 1995	Kakogawa	1107	6.9	1.8314	0.0654
Dinar Turkey, 1995	Dinar	1141	6.4	0.9597	0.084
Kocaeli Turkey, 1999	Duzce	1158	7.51	1.2304	0.0372
Chi-Chi Taiwan, 1999	TCU055	1495	7.62	1.3825	0.0431
Duzce Turkey, 1999	Duzce	1605	7.14	0.8506	0.0988
Taiwan SMART1(45), 1986	SMART1 M04	3674	7.3	1.9297	0.0229
Parkfield-02 CA, 2004	Parkfield - Fault Zone 7	4111	6	1.7026	0.0641
Umbria Marche (foreshock) Italy, 1997	Colfiorito	4337	5.7	1.5799	0.1008
Chuetsu-oki Japan, 2007	Sanjo Shinbori	4860	6.8	1.1128	0.0483
Iwate Japan, 2008	Nakashinden Town	5774	6.9	1.9307	0.0418
El Mayor-Cucapah Mexico, 2010	Calexico Fire Station	5975	7.2	1.6381	0.0265
Darfield New Zealand, 2010	Christchurch Cashmere High School	6890	7	1.4672	0.037
Christchurch New Zealand, 2011	Christchurch Hospital	8066	6.2	0.8965	0.0497

2

3

Table B4: 8S SLS ground motion suite

Earthquake	Station	RSN	Mag.	Scale	MSE
Imperial Valley-02, 1940	El Centro Array #9	6	6.95	0.6652	0.0312
Point Mugu, 1973	Port Hueneme	97	5.65	1.769	0.04
Tabas Iran, 1978	Boshrooyeh	138	7.35	1.796	0.0525
Imperial Valley-06, 1979	Delta	169	6.53	0.7814	0.0331
Victoria Mexico, 1980	Chihuahua	266	6.33	1.096	0.0531
Coalinga-01, 1983	Pleasant Valley P.P. - bldg	367	6.36	0.5572	0.0444
N. Palm Springs, 1986	Palm Springs Airport	530	6.06	1.6566	0.0535
Superstition Hills-02, 1987	El Centro Imp. Co. Cent	721	6.54	0.6498	0.0264
Loma Prieta, 1989	Sunnyvale - Colton Ave.	806	6.93	1.0393	0.0531
Landers, 1992	Indio - Coachella Canal	862	7.28	1.7294	0.0414
Big Bear-01, 1992	San Bernardino - 2nd & Arrowhead	930	6.46	1.8387	0.0485
Northridge-01, 1994	LA - Pico & Sentous	1000	6.69	1.8434	0.0348
Kobe Japan, 1995	Sakai	1115	6.9	1.164	0.0418
Kocaeli Turkey, 1999	Duzce	1158	7.51	0.6192	0.0372
Chi-Chi Taiwan, 1999	TCU098	1526	7.62	1.4854	0.0223
Manjil Iran, 1990	Rudsar	1637	7.37	1.8744	0.0368
Chi-Chi Taiwan-04, 1999	CHY088	2744	6.2	1.8106	0.0494
Chi-Chi Taiwan-06, 1999	CHY039	3277	6.3	1.648	0.019
Taiwan SMART1(40), 1986	SMART1 O02	3653	6.32	1.3647	0.0526
Taiwan SMART1(45), 1986	SMART1 M04	3674	7.3	0.9712	0.0229
Parkfield-02 CA, 2004	PARKFIELD - VINEYARD	4074	6	1.0739	0.027
Chuetsu-oki Japan, 2007	Hinodecho Yoshida Tsubame City	4880	6.8	1.5608	0.0326
Iwate Japan, 2008	Nakashinden Town	5774	6.9	0.9717	0.0418
El Mayor-Cucapah Mexico, 2010	Calexico Fire Station	5975	7.2	0.8244	0.0265
Darfield New Zealand, 2010	Christchurch Cashmere High School	6890	7	0.7384	0.037

1

Table B5: 16S ULS ground motion suite

Earthquake	Station	RSN	Mag.	Scale	MSE
Imperial Valley-02, 1940	El Centro Array #9	6	6.95	1.3436	0.0385
Managua Nicaragua-01, 1972	Managua ESSO	95	6.24	1.7129	0.1068
Imperial Valley-06, 1979	Chihuahua	165	6.53	1.6993	0.0597
Victoria Mexico, 1980	Chihuahua	266	6.33	1.6965	0.1277
Coalinga-01, 1983	Cantua Creek School	322	6.36	1.5789	0.0867
Coalinga-05, 1983	Pleasant Valley P.P. - yard	412	5.77	1.8945	0.108
N. Palm Springs, 1986	North Palm Springs	529	6.06	0.9807	0.0695
Chalfant Valley-02, 1986	Zack Brothers Ranch	558	6.19	1.3714	0.1368
Taiwan SMART1(45), 1986	SMART1 O07	581	7.3	1.7406	0.0543
Superstition Hills-02, 1987	El Centro Imp. Co. Cent	721	6.54	1.1342	0.0476
Loma Prieta, 1989	Hollister - South & Pine	776	6.93	0.6616	0.0135
Northridge-01, 1994	Northridge - 17645 Saticoy St	1048	6.69	1.2503	0.0367
Kobe Japan, 1995	Shin-Osaka	1116	6.9	1.319	0.0541
Dinar Turkey, 1995	Dinar	1141	6.4	0.9108	0.0863
Chi-Chi Taiwan, 1999	ILA013	1317	7.62	1.5504	0.0584
Hector Mine, 1999	Mecca - CVWD Yard	1810	7.13	1.9196	0.1076
Taiwan SMART1(40), 1986	SMART1 O03	3654	6.32	1.896	0.0577
Landers, 1992	Indio - Jackson Road	3754	7.28	1.2324	0.0844
Parkfield-02 CA, 2004	PARKFIELD - 1-STORY SCHOOL	4084	6	1.4336	0.1006
Niigata Japan, 2004	NIG017	4207	6.63	1.2771	0.0472
Chuetsu-oki Japan, 2007	Kashiwazaki NPP Unit 5: ground	4895	6.8	0.6536	0.0162
Iwate Japan, 2008	Misato Miyagi Kitaura - A	5781	6.9	1.8352	0.1556
El Mayor-Cucapah Mexico, 2010	El Centro Array #11	5992	7.2	1.0131	0.0905
Darfield New Zealand, 2010	Kaiapoi North School	6923	7	1.1757	0.105
Christchurch New Zealand, 2011	Papanui High School	8118	6.2	1.2438	0.0358

2

3

Table B6: 16S SLS ground motion suite

Earthquake	Station	RSN	Mag.	Scale	MSE
Imperial Valley-02, 1940	El Centro Array #9	6	6.95	0.6812	0.0385
Parkfield, 1966	Cholame - Shandon Array #5	30	6.19	1.1859	0.0623
Managua Nicaragua-02, 1972	Managua ESSO	96	5.2	1.0238	0.0333
Imperial Valley-06, 1979	Chihuahua	165	6.53	0.8616	0.0597
Westmorland, 1981	Salton Sea Wildlife Refuge	317	5.9	1.4957	0.0347
Coalinga-01, 1983	Parkfield - Fault Zone 7	345	6.36	1.0477	0.044
Morgan Hill, 1984	Gilroy Array #3	457	6.19	1.8027	0.0517
N. Palm Springs, 1986	Desert Hot Springs	517	6.06	0.9851	0.0369
Taiwan SMART1(45), 1986	SMART1 O07	581	7.3	0.8825	0.0543
Superstition Hills-02, 1987	El Centro Imp. Co. Cent	721	6.54	0.575	0.0476
Loma Prieta, 1989	Coyote Lake Dam (Downst)	754	6.93	1.7465	0.0295
Landers, 1992	North Palm Springs	882	7.28	1.4777	0.0354
Big Bear-01, 1992	San Bernardino - E Hospitality	931	6.46	1.4056	0.051
Northridge-01, 1994	Camarillo	958	6.69	1.1836	0.0296
Kobe Japan, 1995	Kakogawa	1107	6.9	1.0177	0.062
Chi-Chi Taiwan, 1999	TAP095	1456	7.62	1.1896	0.0286
Manjil Iran, 1990	Rudsar	1637	7.37	1.8992	0.0432
Chi-Chi Taiwan-06, 1999	CHY037	3276	6.3	1.1374	0.068
Taiwan SMART1(40), 1986	SMART1 O02	3653	6.32	1.2528	0.0219
Parkfield-02 CA, 2004	Parkfield - Vineyard Cany 3W	4134	6	1.3402	0.0427
Niigata Japan, 2004	NIG017	4207	6.63	0.6475	0.0472
Chuetsu-oki Japan, 2007	NIG022	5268	6.8	1.8104	0.0291
Iwate Japan, 2008	Yoneyamacho Tome City	5785	6.9	0.9853	0.077
Darfield New Zealand, 2010	LRSC	6930	7	1.7693	0.0311
Christchurch New Zealand, 2011	Papanui High School	8118	6.2	0.6306	0.0358

4

1

Table B7: 4D ULS ground motion suite

Earthquake	Station	RSN	Mag.	Scale	MSE
Imperial Valley-02, 1940	El Centro Array #9	6	6.95	1.215	0.0243
Managua Nicaragua-01, 1972	Managua ESSO	95	6.24	1.0805	0.052
Imperial Valley-06, 1979	Delta	169	6.53	1.3982	0.027
Westmorland, 1981	Westmorland Fire Sta	319	5.9	1.0142	0.0443
Coalinga-01, 1983	Cantua Creek School	322	6.36	1.7321	0.036
Coalinga-05, 1983	Burnett Construction	405	5.77	1.4346	0.0317
Morgan Hill, 1984	Halls Valley	461	6.19	1.9666	0.0217
Chalfant Valley-02, 1986	Zack Brothers Ranch	558	6.19	0.7454	0.0184
Whittier Narrows-01, 1987	Santa Fe Springs - E.Joslin	692	5.99	0.861	0.0235
Superstition Hills-02, 1987	El Centro Imp. Co. Cent	721	6.54	1.226	0.04
Loma Prieta, 1989	Oakland - Outer Harbor Wharf	783	6.93	1.5169	0.0239
Erzican Turkey, 1992	Erzincan	821	6.69	1.189	0.009
Big Bear-01, 1992	Desert Hot Springs	902	6.46	1.8219	0.0424
Northridge-01, 1994	Canyon Country - W Lost Cany	960	6.69	0.9214	0.0267
Kocaeli Turkey, 1999	Duzce	1158	7.51	1.3036	0.0445
Chi-Chi Taiwan, 1999	CHY036	1203	7.62	1.503	0.0541
Northwest China-03, 1997	Jiashi	1752	6.1	1.442	0.0471
Chi-Chi Taiwan-06, 1999	CHY082	3306	6.3	1.9544	0.0217
Parkfield-02 CA, 2004	PARKFIELD - UPSAR 10	4146	6	1.5226	0.0294
Friuli (aftershock 9) Italy, 1976	Buia	4276	5.5	1.9422	0.0493
Chuetsu-oki Japan, 2007	NIG018	5264	6.8	0.7921	0.0142
Iwate Japan, 2008	Furukawa Osaki City	5814	6.9	1.6951	0.0339
El Mayor-Cucapah Mexico, 2010	Chihuahua	5823	7.2	1.6009	0.0185
Darfield New Zealand, 2010	Kaiapoi North School	6923	7	1.2379	0.0175
Christchurch New Zealand, 2011	Christchurch Botanical Gardens	8063	6.2	0.8137	0.022

2

3

Table B8: 4D SLS ground motion suite

Earthquake	Station	RSN	Mag.	Scale	MSE
Imperial Valley-02, 1940	El Centro Array #9	6	6.95	0.6103	0.0243
Northern Calif-03, 1954	Ferndale City Hall	20	6.5	1.2305	0.0231
Imperial Valley-06, 1979	Delta	169	6.53	0.7024	0.027
Imperial Valley-07, 1979	El Centro Array #2	200	5.01	1.4421	0.0268
Victoria Mexico, 1980	Chihuahua	266	6.33	1.1843	0.0292
Coalinga-02, 1983	TRA (temp)	388	5.09	1.6795	0.0306
Coalinga-05, 1983	Burnett Construction	405	5.77	0.7207	0.0317
Morgan Hill, 1984	Halls Valley	461	6.19	0.9879	0.0217
Taiwan SMART1(45), 1986	SMART1 O08	582	7.3	1.455	0.018
Whittier Narrows-01, 1987	Downey - Co Maint Bldg	615	5.99	0.8958	0.0245
Loma Prieta, 1989	Fremont - Emerson Court	761	6.93	1.3128	0.0136
Erzican Turkey, 1992	Erzincan	821	6.69	0.5973	0.009
Northridge-01, 1994	Manhattan Beach - Manhattan	1035	6.69	1.2251	0.0145
Chi-Chi Taiwan, 1999	TCU098	1526	7.62	1.5974	0.0177
Northridge-06, 1994	Sylmar - Converter Sta	1736	5.28	1.0238	0.0312
Hector Mine, 1999	Baker Fire Station	1766	7.13	1.3799	0.0237
Taiwan SMART1(40), 1986	SMART1 O08	3658	6.32	1.7456	0.0162
Whittier Narrows-02, 1987	Bell Gardens - Jaboneria	3687	5.27	1.6057	0.0195
Chi-Chi Taiwan-06, 1999	CHY002	3863	6.3	1.0203	0.0129
Parkfield-02 CA, 2004	PARKFIELD - 1-STORY SCHOOL	4084	6	0.999	0.0179
Iwate Japan, 2008	Minamikatamachi Tore City	5786	6.9	1.2355	0.0223
El Mayor-Cucapah Mexico, 2010	Chihuahua	5823	7.2	0.8042	0.0185
Tottori Japan, 2000	HRS014	6207	6.61	1.9636	0.0311
Darfield New Zealand, 2010	Kaiapoi North School	6923	7	0.6218	0.0175
Christchurch New Zealand, 2011	LINC	8102	6.2	1.8155	0.0229

4

1

Table B9: 8D ULS ground motion suite

Earthquake	Station	RSN	Mag.	Scale	MSE
Imperial Valley-02, 1940	El Centro Array #9	6	6.95	1.2383	0.0186
Managua Nicaragua-01, 1972	Managua ESSO	95	6.24	1.1713	0.08
Gazli USSR, 1976	Karakyr	126	6.8	0.7137	0.0363
Coalinga-01, 1983	Cantua Creek School	322	6.36	1.5345	0.0312
Coalinga-05, 1983	Burnett Construction	405	5.77	1.6134	0.1098
Morgan Hill, 1984	Gilroy Array #4	458	6.19	1.7154	0.1165
N. Palm Springs, 1986	North Palm Springs	529	6.06	0.7979	0.0993
Chalfant Valley-02, 1986	Zack Brothers Ranch	558	6.19	0.8053	0.0559
Whittier Narrows-01, 1987	Compton - Castlegate St	611	5.99	1.2781	0.0211
Superstition Hills-02, 1987	El Centro Imp. Co. Cent	721	6.54	1.219	0.0388
Loma Prieta, 1989	Palo Alto - 1900 Embarc.	786	6.93	1.3582	0.0554
Erzican Turkey, 1992	Erzincan	821	6.69	1.0137	0.0755
Big Bear-01, 1992	Desert Hot Springs	902	6.46	1.7695	0.0469
Northridge-01, 1994	Arleta - Nordhoff Fire Sta	949	6.69	1.1646	0.0325
Dinar Turkey, 1995	Dinar	1141	6.4	1.0289	0.078
Kocaeli Turkey, 1999	Duzce	1158	7.51	1.2435	0.0384
Chi-Chi Taiwan-03, 1999	TCU065	2618	6.2	1.8394	0.0966
Parkfield-02 CA, 2004	Parkfield - Fault Zone 7	4111	6	1.5491	0.0397
Friuli (aftershock 9) Italy, 1976	Buia	4276	5.5	1.9068	0.0713
Umbria Marche (foreshock) Italy, 1997	Colfiorito	4337	5.7	1.5663	0.0961
Chuetsu-oki Japan, 2007	NIG018	5264	6.8	0.7507	0.0376
Iwate Japan, 2008	Nakashinden Town	5774	6.9	1.8491	0.0497
El Mayor-Cucapah Mexico, 2010	Calexico Fire Station	5975	7.2	1.5748	0.0254
Darfield New Zealand, 2010	Christchurch Cashmere High School	6890	7	1.5213	0.0283
Christchurch New Zealand, 2011	Christchurch Botanical Gardens	8063	6.2	0.783	0.0337

2

3

Table B10: 8D SLS ground motion suite

Earthquake	Station	RSN	Mag.	Scale	MSE
Imperial Valley-02, 1940	El Centro Array #9	6	6.95	0.6256	0.0186
Point Mugu, 1973	Port Hueneme	97	5.65	1.7875	0.0401
Tabas Iran, 1978	Boshrooyeh	138	7.35	1.8216	0.0455
Imperial Valley-06, 1979	Delta	169	6.53	0.7534	0.0365
Victoria Mexico, 1980	Chihuahua	266	6.33	1.1792	0.0387
Coalinga-01, 1983	Cantua Creek School	322	6.36	0.7753	0.0312
Whittier Narrows-01, 1987	Compton - Castlegate St	611	5.99	0.6457	0.0211
Superstition Hills-02, 1987	El Centro Imp. Co. Cent	721	6.54	0.6159	0.0388
Loma Prieta, 1989	Fremont - Emerson Court	761	6.93	1.3878	0.0351
Landers, 1992	Indio - Coachella Canal	862	7.28	1.7487	0.0403
Northridge-01, 1994	LA - Pico & Sentous	1000	6.69	1.841	0.0314
Kobe Japan, 1995	Sakai	1115	6.9	1.1468	0.0437
Kocaeli Turkey, 1999	Zeytinburnu	1177	7.51	1.8932	0.0285
Chi-Chi Taiwan, 1999	TCU098	1526	7.62	1.5123	0.0197
Manjil Iran, 1990	Abhar	1634	7.37	1.2127	0.0356
Chi-Chi Taiwan-03, 1999	CHY101	2507	6.2	1.5163	0.0397
Chi-Chi Taiwan-04, 1999	CHY088	2744	6.2	1.9127	0.0396
Chi-Chi Taiwan-06, 1999	CHY039	3277	6.3	1.746	0.028
Taiwan SMART1(45), 1986	SMART1 M04	3674	7.3	1.0488	0.0298
Whittier Narrows-02, 1987	LA - W 70th St	3717	5.27	1.3924	0.0442
Parkfield-02 CA, 2004	PARKFIELD - VINEYARD	4074	6	1.0396	0.0221
Chuetsu-oki Japan, 2007	Hinodecho Yoshida Tsubame City	4880	6.8	1.5103	0.0377
Iwate Japan, 2008	Takanashi Daisen	5798	6.9	1.4511	0.0447
El Mayor-Cucapah Mexico, 2010	Calexico Fire Station	5975	7.2	0.7956	0.0254
Darfield New Zealand, 2010	Christchurch Cashmere High School	6890	7	0.7686	0.0283

4